

Carbon Dioxide Fixation and Sulfate Sequestration by a Supramolecular Trigonal Bipyramidal

Colm Browne, William J. Ramsay, Tanya K. Ronson, John Medley-Hallam, and Jonathan R. Nitschke*

Abstract: The subcomponent self-assembly of a bent dialdehyde ligand and different cationic and anionic templates led to the formation of two new metallosupramolecular architectures: a $\text{Fe}^{II} \cdot \text{L}_6$ molecular rectangle was isolated following reaction of the ligand with iron(II) tetrafluoroborate, and a M_5L_6 trigonal bipyramidal structure was constructed from either zinc(II) tetrafluoroborate or cadmium(II) trifluoromethanesulfonate. The spatially constrained arrangement of the three equatorial metal ions in the M_5L_6 structures was found to induce small-molecule transformations. Atmospheric carbon dioxide was fixed as carbonate and bound to the equatorial metal centers in both the Zn_5L_6 and Cd_5L_6 assemblies, and sulfur dioxide was hydrated and bound as the sulfite dianion in the Zn_5L_6 structure. Subsequent in situ oxidation of the sulfite dianion resulted in a sulfate dianion bound within the supramolecular pocket.

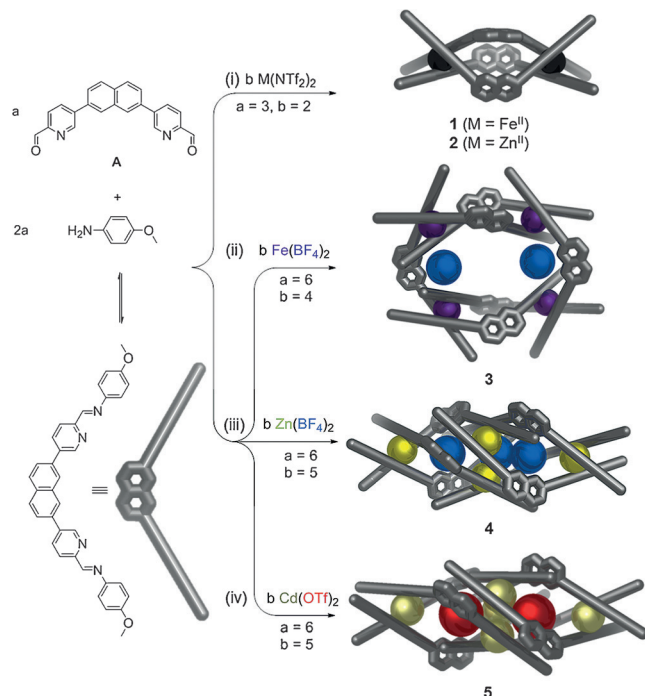
Three-dimensional metal–organic self-assembly allows for the preparation of increasingly intricate structures that contain void spaces.^[1] Valuable understanding is being gained as to how to design and control the chemical environments of these voids, allowing the inner phases of new assemblies to display properties distinct from the solvent environment and enabling selective recognition and transformations of various substrates.^[2]

The combination of multidentate coordinating ligands and metal ions with well-defined coordination spheres, in conjunction with secondary templates such as anions,^[3] has proven to be a powerful construction technique for supramolecular assembly.^[4] The arrangement of the ligands around these templates can generate isolated cavities which have found diverse applications, including in catalysis,^[5] gas storage,^[6] and selective guest binding,^[7] among others.^[8] Minor and subtle variations in ligand design, such as the ligand bend angle,^[9] preferred metal coordination geometry and stoichiometry,^[10] flexibility,^[11] and interactions with the

solvent,^[12] have been shown to be important not only in governing the overall structures formed, but also for defining the physicochemical characteristics of the resulting cavities.

Rules have been established to define the geometric parameters that lead to the formation of metal–organic tetrahedral^[13] or cubic^[14] assemblies, and rational design principles have been put forth to describe the preparation of more complex three-dimensional architectures.^[9a,15] Based upon the understanding gained as these rule sets were deciphered, ligand geometries may be identified wherein the rules do not suggest a clearly defined self-assembly outcome. The design of a rigid ligand that fits one of these geometries may thus allow for serendipity to be engineered^[16] and for new functions to be accessed that are difficult to envisage using rationally designed structures.

Subcomponent **A** (Scheme 1) was prepared in this spirit, as described in the Supporting Information (Section S1.2). The coordination vectors of **A** converge in such a way as to disfavor the formation of a tetrahedron, cube, or polymer,^[17]



Scheme 1. The self-assembly of dialdehyde **A** with *p*-anisidine and i) $\text{M(NTf}_2\text{)}_2$ ($\text{M} = \text{Fe}^{II}$, Zn^{II}) in acetonitrile led to the formation of helicates **1** and **2**, respectively. When ii) $\text{Fe(BF}_4\text{)}_2$, iii) $\text{Zn(BF}_4\text{)}_2$, or iv) Cd(OTf)_2 were employed in the self-assembly procedure, the anions and metal cations cooperatively templated the structures of **3**, **4** and **5**, respectively.

[*] Dr. C. Browne,^{[S][+]} W. J. Ramsay,^[+] Dr. T. K. Ronson, J. Medley-Hallam, Prof. J. R. Nitschke
University of Cambridge, Department of Chemistry
Lensfield Road, Cambridge, CB2 1EW (UK)
E-mail: jrn34@cam.ac.uk
Homepage: <http://www-jrn.ch.cam.ac.uk/>

[+] Current address:
School of Chemistry, University of Manchester
Oxford Road, Manchester, M13 9PL (UK)

[†] These authors contributed equally to this work.

Supporting information for this article is available on the WWW under <http://dx.doi.org/10.1002/anie.201504856>.

and to destabilize a helicate. **A** instead generated a new class of trigonal bipyramidal structures in which a central guest is exposed directly to three dicationic metal centers, allowing for selective transformations and substrate stabilization. **A** was also found to generate a new M_4L_6 molecular rectangle with different templates.

The reaction of iron(II) bis(trifluoromethanesulfonimide) (triflimide, NTf_2^-) or zinc(II) triflimide (2 equiv) with *p*-anisidine (6 equiv) and **A** (3 equiv) in acetonitrile produced M_2L_3 helicate structures **1** or **2**, respectively, as confirmed by NMR spectroscopy and mass spectrometry (Scheme 1; Sections S1.3 and S1.4). Triflimide is known to exercise less influence as a template upon self-assembled metal–organic structures^[18] than smaller noncoordinating anions,^[19] prompting the investigation of tetrafluoroborate (BF_4^-) as an anionic template^[20] in place of triflimide in the system described in Scheme 1.

Although the reaction between **A** (3 equiv), *p*-anisidine (6 equiv), and $Fe(BF_4)_2$ (2 equiv) in acetonitrile produced a deep-blue solution consistent with the formation of **1**, the 1H NMR spectrum of this solution was complex (Supporting Information Figure S6), indicating the formation of a species having lower than expected symmetry. Two distinguishable products were evident by DOSY NMR experiments (Figure S7), with the chemical shifts of the signals for the hydrodynamically smaller species consistent with those of **1** detected when $Fe(NTf_2)_2$ had been used. Signals attributable to helicate **1** were detected by electrospray MS (Figure S8), and the second species was identified as having a metal:ligand ratio of 4:6 (confirmed by HRMS, Figure S9), suggesting the formation of a Fe_4L_6 structure.

Single-crystal X-ray diffraction^[21] revealed the structure of this $Fe^{II}_4L_6$ species **3** (Figure 1). Instead of the tetrahedral arrangement usually observed for M_4L_6 assemblies,^[22] **3** has four Fe^{II} centers arranged into a rectangle. The shorter edges have an average $Fe\cdots Fe$ distance of 11.3 Å and are composed of a single ligand that bridges two metal centers. The longer edges have an average $Fe\cdots Fe$ distance of 13.4 Å and consist

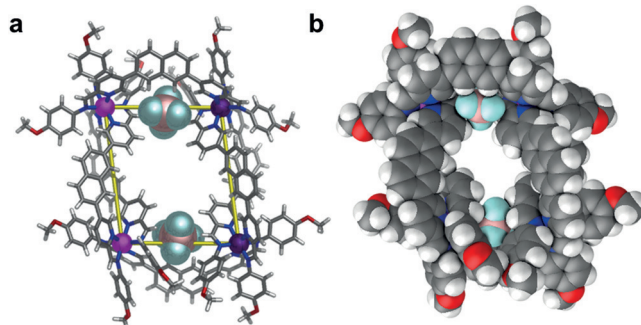


Figure 1. a) Framework representation of the X-ray crystal structure of **3**, where the $2BF_4^-$ ions occupying the binding pockets are shown as a space-filling model. Dark purple spheres correspond to Fe^{II} ions of Δ stereochemistry, and light purple to Λ - Fe^{II} . The edges of the rectangle are highlighted by yellow lines. b) Space-filling representation of **3**, highlighting the tight arrangement of the ligands around the BF_4^- ions. Atom colors: C=gray, N=blue, Fe=purple, H=white, F=cyan, B=pink, O=red. Disorder, non-encapsulated anions, and solvent molecules are omitted for clarity.

of two intertwined ligands, forming a double-stranded helix. Each helix within the rectangle bridges two metal centers with identical handedness, with each helical edge mirroring the other's handedness (Figure 1a). All metal centers have *mer* coordination geometry, in contrast to the *fac* geometry usually found in M_4L_6 tetrahedra.^[23] The arrangement of the ligands defines a binding pocket at each of the shorter rectangular edges, each of which binds a BF_4^- ion (Figure 1b); the distances between the protons of the ligand and the BF_4^- ions (2.24–2.63 Å) are within the expected range for CH···F hydrogen bonds.^[24] Resonances in the ^{19}F NMR spectrum suggested that this interaction also existed in solution, in fast exchange on the NMR timescale (Figure S10). We attribute the stability of **3** to a combination of anion templation and aromatic stacking.^[3c,25]

Prompted by the novel structure of **3** templated by the BF_4^- ion, we investigated the reaction of **A**, *p*-anisidine, and $Zn(BF_4)_2$ in a 3:6:2 ratio in acetonitrile (Section S1.6). The 1H NMR spectrum of the reaction mixture was again more complex than that detected for helicate **2**, and signals corresponding to excess ligand were detected (Figure S13A). However, DOSY NMR of the purified product gave results consistent with the formation of a single species (Figure S14). Single-crystal X-ray analysis revealed the presence of an unusual Zn_5L_6 trigonal bipyramidal^[26] **4** (Figure 2).

The structure of **4** contains two Zn^{II} ions of identical handedness and *fac* stereochemistry at the two apical vertices (both enantiomers are present in the unit cell) and three Zn^{II} ions in equatorial positions. The Zn_5L_6 framework displays approximate D_3 symmetry but the crystal structure of **4** is C_1 symmetric because of the coordination environments of the equatorial metal centers. The $Zn\cdots Zn$ distance

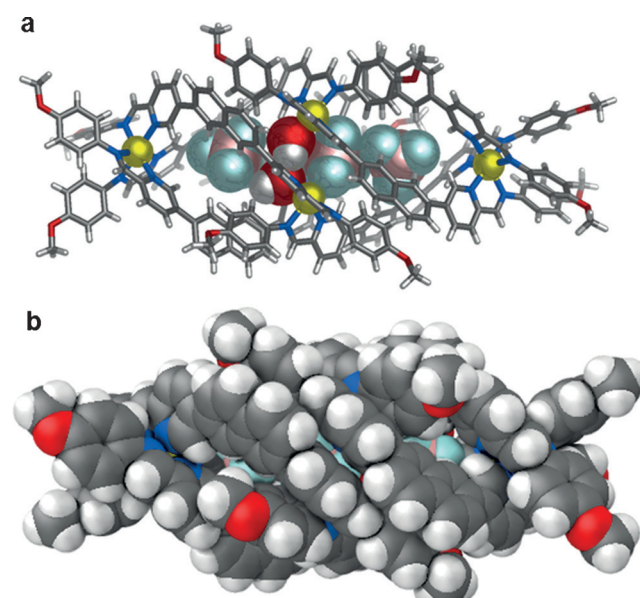


Figure 2. a) Framework representation of the X-ray crystal structure of **4**, where the BF_4^- and hydroxide ions occupying the cavity are shown in space-filling mode. b) The space-filling representation of **4** highlights the aromatic stacking of the ligands. Atom colors: C=gray, N=blue, Zn=yellow, H=white, F=cyan, B=pink, O=red. Disorder, non-encapsulated anions, and solvent molecules are omitted for clarity.

between apical sites is 21.2 Å, and the Zn^{II}–Zn distances at the equatorial positions range from 5.07 to 5.18 Å. The ligands forming the edges of the trigonal bipyramidal exhibit extensive face-to-face aromatic stacking (Figure 2b), defining two separate cavities that are separated by the equatorial ring of Zn^{II} centers. A BF₄⁻ ion is bound in each binding pocket, stabilized by attractive electrostatic forces and CH···F hydrogen-bonding interactions with the protons lining the interior of the binding pocket. An analysis of the ¹⁹F NMR spectrum revealed that the bound BF₄⁻ ions were in slow exchange on the NMR timescale in solution (Figure S15), with correlations to inward-facing host protons detected in the ¹⁹F-¹H HOESY spectrum (Figure S16). A third BF₄⁻ ion is bound at the equator of **4** and acts as a tris(monodentate) ligand,^[27] bridging the three equatorial Zn^{II} centers with three of its fluorine atoms. Two of these Zn^{II} ions are each coordinated to an additional hydroxide ion; the equatorial belt thus consists of two six-coordinate Zn^{II} centers and one five-coordinate Zn^{II} ion. Several combinations of water, hydroxide, and acetonitrile adducts were detected in the HRMS spectrum after dissolving the crystals of **4** in acetonitrile (Figure S19), suggesting dynamic exchange of these weakly bound ligands at the equatorial positions in solution. This is consistent with the multiple environments evident in the complex ¹H NMR spectrum of **4**, with different signal intensities reflecting slight preferences for the formation of some adducts over others.

As a result of the similar geometric preferences of Cd^{II} and Zn^{II} ions,^[28] we anticipated that a similar M₅L₆ trigonal bipyramidal structure would self-assemble upon reaction of **A**, *p*-anisidine, and cadmium(II) trifluoromethanesulfonate (OTf⁻; Section S1.7). The ¹H NMR spectrum of this solution was broad, with multiple signals for each proton, similar to that of **4** (Figure S20). Single-crystal X-ray diffraction revealed the structure of trigonal bipyramid **5** (Figure 3).

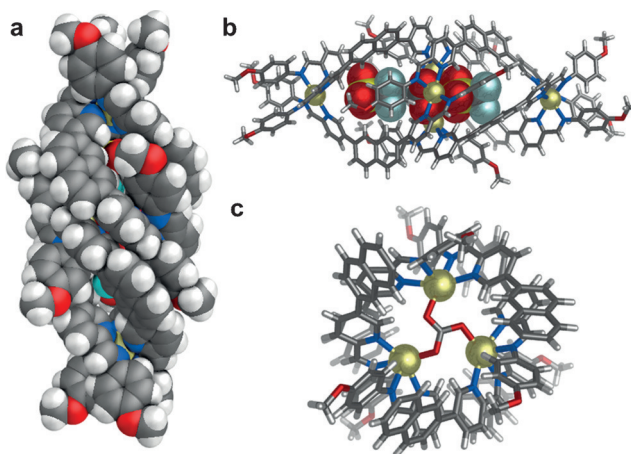


Figure 3. a) Space-filling representation of the X-ray crystal structure of **5**, where b) two OTf⁻ ions (shown in space-filling model) occupy the two binding pockets of **5** (shown as a framework). c) View down the long axis of the structure showing coordination of a carbonate ion to the equatorial Cd^{II} centers (apical metal centers are omitted for clarity). Atom colors: C = gray, N = blue, Cd = light yellow, H = white, F = light blue, B = pink, O = red, S = dark yellow. Disorder, non-encapsulated anions, and solvent molecules are omitted for clarity.

The distance between the apical Cd centers in **5** is 21.9 Å, with 4.74–5.06 Å between the equatorial centers, resulting in a longer and narrower trigonal bipyramidal in comparison to **4**. One of the encapsulated OTf⁻ ions shows CH···F and CH···O^[29] interactions, which likely contribute both to guest binding and host stability. The second cavity is also occupied by a OTf⁻ ion, which is bound as a tris(monodentate) ligand bridging between the three equatorial Cd^{II} centers through its oxygen atoms (Figure 3b). Intriguingly, the octahedral coordination sphere of the equatorial Cd^{II} centers is satisfied by a carbonate dianion, which forms three bonds to the equatorial metal centers with its oxygen atoms (Figure 3c). The C–O bond lengths of 1.26(1)–1.30(1) Å are in good agreement for those expected for carbonate.^[30] The poor solubility of the crystals of **5** hindered NMR characterization and the investigation of carbonate binding in solution, but signals detected in the mass spectrum of **5** were consistent with carbonate binding in solution (Figure S21). As no carbonate was added to the solution during the self-assembly of **5**, we infer that the anion was generated from atmospheric carbon dioxide;^[31] if self-assembly occurred under a nitrogen atmosphere, **5** was not observed to form.

To better understand the carbonate binding abilities of this new trigonal-bipyramidal structure type, further studies focused upon the structurally similar compound **4** because of the better solubility of this structure (Section S3.1).

When **4** self-assembled from its subcomponents under a N₂ atmosphere, ESI-MS identified the presence of the trigonal bipyramidal but extended heating did not yield any changes (Figure S22). However, when this sample was exposed to air and heated at 70°C for an additional 48 h, new signals corresponding to a carbonate adduct of **4** were detected by mass spectrometry (Figures S22, S23). This observation suggested that **4** was capable of binding CO₂ as CO₃²⁻ in a similar manner to **5**. After seven days at 70°C the intensities of these new signals (relative to the carbonate-free form) in the mass spectrum were found to increase, which we inferred to result from an increase in CO₃²⁻ concentration in solution; only a slight broadening of the signals of **4** in the ¹H NMR spectrum was detected during this transformation (Figure S24).

When helicate **2** was kept at room temperature open to air for four weeks, no evidence of carbonate binding was evident in the ¹H NMR (Figure S25) or mass spectra (Figure S26). When excess Me₄N⁺BF₄⁻ (10 equiv) was added to a solution of **2**, the resonance signals in the ¹H NMR spectrum of **2** immediately shifted, with the greatest change detected for the protons orientated towards the interior of **2**. Models suggest that the cavity of **2** is sufficiently large for BF₄⁻ encapsulation (Figure S27). A single ¹⁹F NMR resonance signal, shifted upfield with respect to free BF₄⁻, was detected, suggesting that BF₄⁻ ions were in fast exchange with the cavity of **2** in solution (Figure S28). ESI-MS also provided evidence consistent with host–guest binding (Figure S29).

Under air over a two week period, the signals attributed to [BF₄⁻•**2**] in the ¹H NMR spectrum decreased in intensity, with concomitant growth of new, broad signals, which were comparable to the ¹H NMR spectrum of **4**. ESI-MS results were consistent with the formation of trigonal bipyramid **4**.

containing bound carbonate (Figure S29). These observations suggest that the cavity of **4** must first be opened through BF_4^- or OTf^- templation before CO_2 fixation may occur.

Based on the observation that **4** and **5** were capable of fixing carbon dioxide as carbonate in solution, we hypothesized that similar small-molecule capture might be possible with sulfur dioxide (Section S3.2). When a solution of sulfur dioxide in water was added to the subcomponents necessary for the formation of **4** in acetonitrile in air, ESI-MS signals were detected consistent with the formation of the sulfite (SO_3^{2-}) adduct of **4** after 25 min stirring at 70°C (Figures S30, S31). Sulfate (SO_4^{2-}) was present in the sulfur dioxide solution as an impurity (approximately 18%); MS signals corresponding to **4** with two equivalents of SO_4^{2-} were also detected (Figure S32). After 25 min, the relative intensities of the signals for the SO_4^{2-} adduct of **4** in comparison to those of the SO_3^{2-} analogue were higher than those detected in a control experiment monitoring sulfite oxidation (Figure S30), suggesting that a SO_4^{2-} guest was preferred over SO_3^{2-} . The rate of decrease in the intensity of the MS signals attributed to the SO_3^{2-} adduct, and the concomitant increase in the signals for the SO_4^{2-} adduct, was consistent with a zero-order rate of reaction in $[\text{SO}_3^{2-}]$, as has been previously reported^[32] (Figures S30b and c). Single-crystal X-ray diffraction revealed the binding of one SO_4^{2-} anion between the equatorial metal sites (Figure 4).

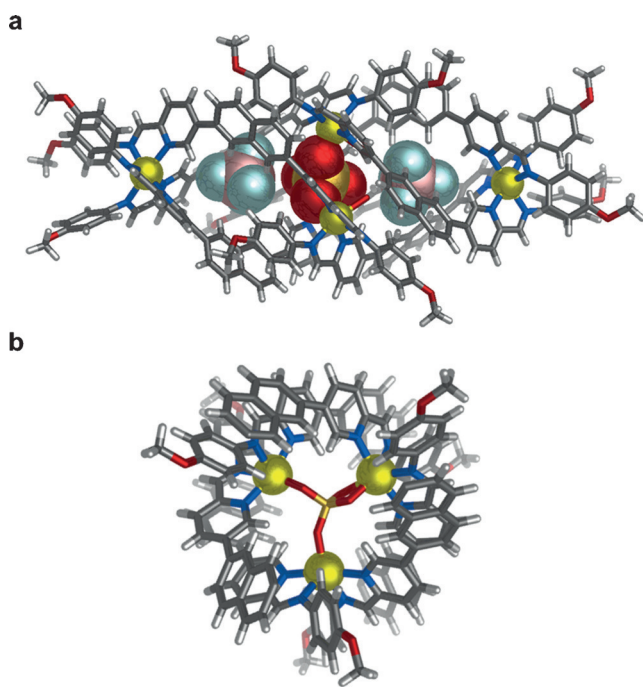


Figure 4. X-ray crystal structure of the sulfate adduct of **4** showing a) the bound anions (sulfate and tetrafluoroborate) in space-filling mode within the framework of **4**, shown in wireframe representation. b) View highlighting the chelation of the centrally bound sulfate by the three equatorial Zn^{II} centers (apical metal centers are removed for clarity). Atom colors: C=gray, N=blue, Zn=yellow, H=white, F=light blue, B=pink, O=red, S=dark yellow. Non-encapsulated anions and solvent molecules are omitted for clarity.

X-ray diffraction analysis indicated that two oxygen donors from the bound sulfate dianion chelate one equatorial Zn^{II} metal center and the remaining two Zn^{II} sites each coordinate to one oxygen from sulfate and to a water molecule. Dissolution of the crystals in acetonitrile yielded a ^1H NMR spectrum with sharp signals (Figure S33), suggesting that this anion was bound more strongly than the previously detected carbonate or hydroxide anions. Peaks attributable to bound carbonate in the ESI mass spectra were not detected after bubbling CO_2 through a solution of the SO_4^{2-} adduct of **4** at 70°C over a two week period (Figure S34). Two signals for BF_4^- were evident in the ^{19}F NMR spectrum (Figure S35), attributable to bound and unbound anions, with a $^{19}\text{F}-^1\text{H}$ HOESY indicating proximity between the tetrafluoroborate anion and the inward-facing protons of **4** (Figure S37). We infer that the rate-limiting step of sulfite oxidation occurs outside of the cavity of **4**, given that no difference was detected between oxidation rates in the presence and absence of the host.

In conclusion, the acute coordination vectors of ligands derived from dialdehyde **A** have allowed for the construction of two new metal–organic structure types, an M_4L_6 rectangle and an M_5L_6 trigonal bipyramidal. The trigonal bipyramidal is capable of fixing carbon dioxide as carbonate and sulfur dioxide as (oxidized) sulfate. Investigations are underway to stabilize a variety of unstable anionic species using this trigonal bipyramidal structure.

Acknowledgements

This work was supported by the EU FP7 Marie Curie Academic-Industrial Initial Training Network on Dynamic Molecular Nanostructures (DYNAMOL; to C.B. and W.J.R.) and the UK Engineering and Physical Sciences Research Council (EPSRC). We thank the Diamond Light Source (UK) for synchrotron beamtime on I19 (MT8464), the NMR facility at the Department of Chemistry, University of Cambridge, and the EPSRC UK National Mass Spectrometry Facility at Swansea University.

Keywords: carbon dioxide fixation · host–guest systems · small-molecule transformations · supramolecular chemistry · template synthesis

How to cite: *Angew. Chem. Int. Ed.* **2015**, *54*, 11122–11127
Angew. Chem. **2015**, *127*, 11274–11279

- [1] T. R. Cook, P. J. Stang, *Chem. Rev.* **2015**, DOI: 10.1021/cr5005666.
- [2] a) A. W. Kleij, J. N. H. Reek, *Chem. Eur. J.* **2006**, *12*, 4218–4227; b) G. H. Clever, *Molecules at Work*, Wiley-VCH, Weinheim, **2012**, pp. 13–37; c) M. J. Hardie, *Chem. Soc. Rev.* **2010**, *39*, 516–527; d) M. Albrecht, *Activating Unreactive Substrates*, Wiley-VCH, Weinheim, **2009**, pp. 411–425; e) M. Yoshizawa, J. K. Klosterman, M. Fujita, *Angew. Chem. Int. Ed.* **2009**, *48*, 3418–3438; *Angew. Chem.* **2009**, *121*, 3470–3490.
- [3] a) N. Gimeno, R. Vilar, *Coord. Chem. Rev.* **2006**, *250*, 3161–3189; b) R. M. Meudtner, S. Hecht, *Angew. Chem. Int. Ed.* **2008**, *47*, 4926–4930; *Angew. Chem.* **2008**, *120*, 5004–5008; c) I. A. Riddell, M. M. J. Smulders, J. K. Clegg, Y. R. Hristova, B.

- Breiner, J. D. Thoburn, J. R. Nitschke, *Nat. Chem.* **2012**, *4*, 751–756; d) H. T. Chifotides, I. D. Giles, K. R. Dunbar, *J. Am. Chem. Soc.* **2013**, *135*, 3039–3055.
- [4] a) R. Chakrabarty, P. S. Mukherjee, P. J. Stang, *Chem. Rev.* **2011**, *111*, 6810–6918; b) D. Fiedler, D. H. Leung, R. G. Bergman, K. N. Raymond, *Acc. Chem. Res.* **2005**, *38*, 349–358; c) M. D. Ward, *Chem. Commun.* **2009**, 4487–4499; d) P. Ballester, *Chem. Soc. Rev.* **2010**, *39*, 3810–3830; e) G. M. Whitesides, B. Grzybowski, *Science* **2002**, *295*, 2418–2421; f) T. K. Ronson, S. Zarra, S. P. Black, J. R. Nitschke, *Chem. Commun.* **2013**, *49*, 2476–2490.
- [5] a) Z. J. Wang, C. J. Brown, R. G. Bergman, K. N. Raymond, F. D. Toste, *J. Am. Chem. Soc.* **2011**, *133*, 7358–7360; b) Y. Kohyama, T. Murase, M. Fujita, *J. Am. Chem. Soc.* **2014**, *136*, 2966–2969.
- [6] a) G. Zhang, O. Presly, F. White, I. M. Oppel, M. Mastalerz, *Angew. Chem. Int. Ed.* **2014**, *53*, 5126–5130; *Angew. Chem.* **2014**, *126*, 5226–5230; b) M. A. Little, M. E. Briggs, J. T. A. Jones, M. Schmidtmann, T. Hasell, S. Y. Chong, K. E. Jelfs, L. Chen, A. I. Cooper, *Nat. Chem.* **2015**, *7*, 153–159; c) I. A. Riddell, M. M. J. Smulders, J. K. Clegg, J. R. Nitschke, *Chem. Commun.* **2011**, *47*, 457–459.
- [7] a) O. Chepelin, J. Ujma, X. Wu, A. M. Z. Slawin, M. B. Pitak, S. J. Coles, J. Michel, A. C. Jones, P. E. Barran, P. J. Lusby, *J. Am. Chem. Soc.* **2012**, *134*, 19334–19337; b) T. Heinz, D. M. Rudkevich, J. Rebek, *Nature* **1998**, *394*, 764–766; c) S. Mirtschin, A. Slabon-Turski, R. Scopelliti, A. H. Velders, K. Severin, *J. Am. Chem. Soc.* **2010**, *132*, 14004–14005; d) Y. Li, A. H. Flood, *J. Am. Chem. Soc.* **2008**, *130*, 12111–12122; e) R. Custelcean, P. V. Bonnesen, N. C. Duncan, X. Zhang, L. A. Watson, G. Van Berk, W. B. Parson, B. P. Hay, *J. Am. Chem. Soc.* **2012**, *134*, 8525–8534; f) S. K. Samanta, M. Schmittel, *Org. Biomol. Chem.* **2013**, *11*, 3108–3115; g) S. Liu, A. D. Shukla, S. Gadde, B. D. Wagner, A. E. Kaifer, L. Isaacs, *Angew. Chem. Int. Ed.* **2008**, *47*, 2657–2660; *Angew. Chem.* **2008**, *120*, 2697–2700; h) G. H. Clever, S. Tashiro, M. Shionoya, *Angew. Chem. Int. Ed.* **2009**, *48*, 7010–7012; *Angew. Chem.* **2009**, *121*, 7144–7146.
- [8] a) Y. Ahn, Y. Jang, N. Selvapalam, G. Yun, K. Kim, *Angew. Chem. Int. Ed.* **2013**, *52*, 3140–3144; *Angew. Chem.* **2013**, *125*, 3222–3226; b) D. Ray, J. T. Foy, R. P. Hughes, I. Aprahamian, *Nat. Chem.* **2012**, *4*, 757–762.
- [9] a) Q.-F. Sun, J. Iwasa, D. Ogawa, Y. Ishido, S. Sato, T. Ozeki, Y. Sei, K. Yamaguchi, M. Fujita, *Science* **2010**, *328*, 1144–1147; b) M. Han, R. Michel, G. H. Clever, *Chem. Eur. J.* **2014**, *20*, 10640–10644; c) T. Weilandt, U. Kiehne, J. Bunzen, G. Schnakenburg, A. Lützen, *Chem. Eur. J.* **2010**, *16*, 2418–2426.
- [10] C. Schouwey, J. J. Holstein, R. Scopelliti, K. O. Zhurov, K. O. Nagornov, Y. O. Tsypin, O. S. Smart, G. Bricogne, K. Severin, *Angew. Chem. Int. Ed.* **2014**, *53*, 11261–11265; *Angew. Chem.* **2014**, *126*, 11443–11447.
- [11] A. Stephenson, M. D. Ward, *Dalton Trans.* **2011**, *40*, 10360–10369.
- [12] Y. Okazawa, K. Kondo, M. Akita, M. Yoshizawa, *J. Am. Chem. Soc.* **2015**, *137*, 98–101.
- [13] a) R. W. Saalfrank, A. Stark, M. Bremer, H.-U. Hummel, *Angew. Chem. Int. Ed. Engl.* **1990**, *29*, 311–314; *Angew. Chem.* **1990**, *102*, 292–295; b) R. W. Saalfrank, H. Glaser, B. Demleitner, F. Hampel, M. M. Chowdhry, V. Schünemann, A. X. Trautwein, G. B. M. Vaughan, R. Yeh, A. V. Davis, K. N. Raymond, *Chem. Eur. J.* **2002**, *8*, 493–497; c) D. L. Caulder, K. N. Raymond, *Acc. Chem. Res.* **1999**, *32*, 975–982.
- [14] a) C. Browne, S. Brenet, J. K. Clegg, J. R. Nitschke, *Angew. Chem. Int. Ed.* **2013**, *52*, 1944–1948; *Angew. Chem.* **2013**, *125*, 1998–2002; b) D. Luo, X.-P. Zhou, D. Li, *Angew. Chem. Int. Ed.* **2015**, *54*, 6190–6195; c) Q.-G. Zhai, C. Mao, X. Zhao, Q. Lin, F. Bu, X. Chen, X. Bu, P. Feng, *Angew. Chem. Int. Ed.* **2015**, *54*, 7884–7888; *Angew. Chem.* **2015**, *127*, 7997–8001; d) P. A. Berseth, J. J. Sokol, M. P. Shores, J. L. Heinrich, J. R. Long, *J. Am. Chem. Soc.* **2000**, *122*, 9655–9662.
- [15] a) K. S. Chichak, S. J. Cantrill, A. R. Pease, S.-H. Chiu, G. W. V. Cave, J. L. Atwood, J. F. Stoddart, *Science* **2004**, *304*, 1308–1312; b) J.-F. Ayme, J. E. Beves, C. J. Campbell, D. A. Leigh, *Angew. Chem. Int. Ed.* **2014**, *53*, 7823–7827; *Angew. Chem.* **2014**, *126*, 7957–7961; c) D. A. Leigh, R. G. Pritchard, A. J. Stephens, *Nat. Chem.* **2014**, *6*, 978–982; d) C. S. Wood, T. K. Ronson, A. M. Belenguer, J. J. Holstein, J. R. Nitschke, *Nat. Chem.* **2015**, *7*, 354–358.
- [16] R. W. Saalfrank, H. Maid, A. Scheurer, *Angew. Chem. Int. Ed.* **2008**, *47*, 8794–8824; *Angew. Chem.* **2008**, *120*, 8924–8956.
- [17] a) M. Burnworth, L. Tang, J. R. Kumpfer, A. J. Duncan, F. L. Beyer, G. L. Fiore, S. J. Rowan, C. Weder, *Nature* **2011**, *472*, 334–337; b) J. R. Kumpfer, S. J. Rowan, *ACS Macro Lett.* **2012**, *1*, 882–887.
- [18] I. A. Riddell, T. K. Ronson, J. K. Clegg, C. S. Wood, R. A. Bilbeisi, J. R. Nitschke, *J. Am. Chem. Soc.* **2014**, *136*, 9491–9498.
- [19] a) V. Amendola, L. Fabbrizzi, *Chem. Commun.* **2009**, 513–531; b) K. M. Mullen, P. D. Beer, *Chem. Soc. Rev.* **2009**, *38*, 1701–1713; c) P. A. Gale, N. Busschaert, C. J. E. Haynes, L. E. Karagiannidis, I. L. Kirby, *Chem. Soc. Rev.* **2014**, *43*, 205–241; d) G. O. Lloyd, J. W. Steed, *Nat. Chem.* **2009**, *1*, 437–442.
- [20] a) L. Raehm, L. Mimassi, C. Guyard-Duhayon, H. Amouri, M. N. Rager, *Inorg. Chem.* **2003**, *42*, 5654–5659; b) H. Amouri, L. Mimassi, M. N. Rager, B. E. Mann, C. Guyard-Duhayon, L. Raehm, *Angew. Chem. Int. Ed.* **2005**, *44*, 4543–4546; *Angew. Chem.* **2005**, *117*, 4619–4622; c) H. Amouri, C. Desmarests, A. Bettoschi, M. N. Rager, K. Boubekeur, P. Rabu, M. Drillon, *Chem. Eur. J.* **2007**, *13*, 5401–5407; d) C. Desmarests, C. Policar, L.-M. Chamoreau, H. Amouri, *Eur. J. Inorg. Chem.* **2009**, 4396–4400; e) S. Freye, J. Hey, A. Torras-Galán, D. Stalke, R. Herbst-Irmer, M. John, G. H. Clever, *Angew. Chem. Int. Ed.* **2012**, *51*, 2191–2194; *Angew. Chem.* **2012**, *124*, 2233–2237; f) C. Klein, C. Gütz, M. Bogner, F. Topić, K. Rissanen, A. Lützen, *Angew. Chem. Int. Ed.* **2014**, *53*, 3739–3742; *Angew. Chem.* **2014**, *126*, 3814–3817; g) D. A. Safin, A. Pialat, A. A. Leitch, N. A. Tumanov, I. Korobkov, Y. Filinchuk, J. L. Brusso, M. Murugesu, *Chem. Commun.* **2015**, *51*, 9547–9550; h) I. A. Riddell, Y. R. Hristova, J. K. Clegg, C. S. Wood, B. Breiner, J. R. Nitschke, *J. Am. Chem. Soc.* **2013**, *135*, 2723–2733.
- [21] a) H. Nowell, S. A. Barnett, K. E. Christensen, S. J. Teat, D. R. Allan, *J. Synchrotron Radiat.* **2012**, *19*, 435–441; b) CCDC 1400514, 1400515, 1400516, 1400517 contain the supplementary crystallographic data for this paper. These data can be obtained free of charge from The Cambridge Crystallographic Data Centre.
- [22] a) A. M. Castilla, W. J. Ramsay, J. R. Nitschke, *Chem. Lett.* **2014**, *43*, 256–263; b) R. W. Saalfrank, B. Hörner, D. Stalke, J. Salbeck, *Angew. Chem. Int. Ed. Engl.* **1993**, *32*, 1179–1182; *Angew. Chem.* **1993**, *105*, 1223–1225; c) P. Mal, D. Schultz, K. Beyeh, K. Rissanen, J. R. Nitschke, *Angew. Chem. Int. Ed.* **2008**, *47*, 8297–8301; *Angew. Chem.* **2008**, *120*, 8421–8425; d) D. L. Caulder, K. N. Raymond, *J. Chem. Soc. Dalton Trans.* **1999**, 1185–1200.
- [23] B. R. Hall, H. Adams, M. D. Ward, *Supramol. Chem.* **2012**, *24*, 499–507.
- [24] F. Grepioni, G. Cojazzi, S. M. Draper, N. Scully, D. Braga, *Organometallics* **1998**, *17*, 296–307.
- [25] Z. R. Bell, J. C. Jeffery, J. A. McCleverty, M. D. Ward, *Angew. Chem. Int. Ed.* **2002**, *41*, 2515–2518; *Angew. Chem.* **2002**, *114*, 2625–2628.
- [26] a) S. Hiraoka, Y. Sakata, M. Shionoya, *J. Am. Chem. Soc.* **2008**, *130*, 10058–10059; b) J. C. Garrison, M. J. Panzner, P. D. Custer, D. V. Reddy, P. L. Rinaldi, C. A. Tessier, W. J. Youngs, *Chem. Commun.* **2006**, 4644–4646; c) S. Cardona-Serra, E. Coronado, P. Gavina, J. Ponce, S. Tatay, *Chem. Commun.* **2011**, *47*, 8235–

- 8237; d) C. J. Kuehl, Y. K. Kryschko, U. Radhakrishnan, S. R. Seidel, S. D. Huang, P. J. Stang, *Proc. Natl. Acad. Sci. USA* **2002**, *99*, 4932–4936; e) M. Wang, C. Wang, X.-Q. Hao, X. Li, T. J. Vaughn, Y.-Y. Zhang, Y. Yu, Z.-Y. Li, M.-P. Song, H.-B. Yang, X. Li, *J. Am. Chem. Soc.* **2014**, *136*, 10499–10507.
- [27] a) L. Alvarado, C. Brewer, G. Brewer, R. J. Butcher, A. Straka, C. Viragh, *CrystEngComm* **2009**, *11*, 2297–2307; b) J. Olguín, M. Kalisz, R. Clérac, S. Brooker, *Inorg. Chem.* **2012**, *51*, 5058–5069; c) N. K. Szymczak, L. A. Berben, J. C. Peters, *Chem. Commun.* **2009**, 6729–6731.
- [28] W. Meng, T. K. Ronson, J. K. Clegg, J. R. Nitschke, *Angew. Chem. Int. Ed.* **2013**, *52*, 1017–1021; *Angew. Chem.* **2013**, *125*, 1051–1055.
- [29] T. Steiner, *Chem. Commun.* **1997**, 727–734.
- [30] H. Effenberger, K. Mereiter, J. Zemann, *Z. Kristallogr.* **1981**, *156*, 233–243.
- [31] a) S. K. Dey, R. Chutia, G. Das, *Inorg. Chem.* **2012**, *51*, 1727–1738; b) S. J. Brooks, P. A. Gale, M. E. Light, *Chem. Commun.* **2006**, 4344–4346; c) T. Gunnlaugsson, P. E. Kruger, P. Jensen, F. M. Pfeffer, G. M. Hussey, *Tetrahedron Lett.* **2003**, *44*, 8909–8913.
- [32] V. Linek, V. Vacek, *Chem. Eng. Sci.* **1981**, *36*, 1747–1768.

Received: May 28, 2015

Published online: July 31, 2015